Scutellarin acts on the AR-NOX Axis to Remediate Oxidative Stress Injury in a Mouse Model of Cerebral Ischemia/Reperfusion Injury

Llin Peng
Guangzhou University of Chinese Medicine https://orcid.org/0000-0001-9621-4203
Minzhen Deng
Guangdong Provincial Hospital of Traditional Chinese Medicine
Yan Huang
Guangdong Provincial Hospital of Traditional Chinese Medicine
Shuang Wu
Guangzhou University of Chinese Medicine
Yucheng Cao
Guangzhou University of Chinese Medicine
Zhijie Gao
Guangzhou University of Chinese Medicine
Xiaoli Wu
Guangdong Provincial Hospital of Traditional Chinese Medicine
Lihua Zhou
Sun Yat-Sen University
Sookja Kim Chung
Macau University of Science and Technology
Jingbo Sun
Guangdong Provincial Hospital of Traditional Chinese Medicine
Xiao Cheng (chengxiaolucky@126.com)
Guangdong Provincial Hospital of Traditional Chinese Medicine

Research

Keywords: Scutellarin, aldose reductase, NADPH oxidase, oxidative stress, ischemia-reperfusion, Quantitative proteomic analysis

Posted Date: May 7th, 2021

DOI: https://doi.org/10.21203/rs.3.rs-471790/v1

Abstract

Backbround

Oxidative stress plays an important role in the ischemic stroke induced brain damage. Our previous study showed that Scutellarin protects against ischemic injury in vitro and in vivo induced oxidative damage in rats, and we also reported that the involvement of Aldose reductase (AR) in oxidative stress and cerebral ischemic injury, in this study we furtherly explicit whether the antioxidant effect of Scutellarin on cerebral ischemia injury is related to AR gene regulation and its specific mechanism.

Methods

C57BL/6N mice (Wild-type, WT) and AR knockout (AR-/-) mice were subjected to transient middle cerebral artery occlusion (tMCAO) model with 1h occlusion followed by 3d reperfusion, and Scutellarin was administered from 2h before surgery to 3 days after surgery. Subsequently, Neurological function were assessed by the modified Longa score method, the histopathological morphology observed with 2,3,5-triphenyltetrazolium chloride and hematoxylin-eosin staining. Enzyme-linked immunosorbent assay was used to detect the levels of ROS, 4-hydroxynonenal (4-HNE), 8-hydroxydeoxyguanosine (8-OHDG), Neurotrophin-3 (NT-3), poly ADP-ribose polymerase-1 (PARP1) and 3-nitrotyrosine (3-NT) in the ischemic penumbra regions. Quantitative proteomics profiling using quantitative nano-HPLC-MS/MS were performed to compare the protein expression difference between AR-/- and WT mice with or without tMCAO injury. The expression of AR, NOX1, NOX2 and NOX4 in the ipsilateral side of ischemic brain were detected by Real time-PCR, Western blot and immunofluorescence co-staining with NeuN.

Results

Scutellarin treatment alleviated brain damage suffered from tMCAO injury such as improved neurological function deficit, brain infarct area and neuronal injury and reduced the expression of oxidation-related products, moreover, also down-regulated tMCAO induced AR mRNA and protein expression.

Conclusions

Scutellarin would be a potential drug for the treatment of ischemic stroke through regulating AR-NOX Axis modulate oxidative stress injury to play the protective role of cerebral ischemia injury.

Introduction

Cerebral ischemia-reperfusion injury is one of the pathological characteristics of many cerebrovascular diseases [1]. Severe cerebral ischemia-reperfusion injury which occurs during an ischemic stroke can produce irreversible ischemic nervous tissue damage in a short time [2]. Long-term cerebral ischemia can ignite an inflammatory response and amino acid toxicity, resulting in cascade of reactions leading to cerebral infarction and neuronal apoptosis [3–7]. In addition, after the cerebral ischemia-reperfusion injury occurs the increased inflammation and oxidative stress damages to the blood-brain barrier leading

to augmented vascular permeability and brain edema [8]. To date, due to multifunctional complex mechanisms of cerebral ischemia injury, there is a critical need for finding the effective therapeutic strategies to explore the protective agents and methods.

In recent years, it is widely believed that there are neuroprotective possibilities of natural compounds extracted from plants against cerebral ischemia injury. These natural agents with the anti-inflammatory, anti-oxidative, anti-apoptotic, and neurofunctional regulatory properties exhibit preventive or therapeutic effects against brain damage [9]. Erigeron breviscapus (Vant.) Hand-Mazz. is a plant species in the Compositae family, findings have indicated that Erigeron breviscapus improves cardiovascular and cerebrovascular function, and that one of its ingredients, scutellarin, has potential value in the treatment of Alzheimer's disease, cancer, diabetic vascular complications, and other conditions [10, 11]. Several studies have reported that Scutellarin has anti-oxidative actions in several disease model such as cerebral ischemia injury and abilities in learning and memory [12–14]. Our previous study indicated that Scutellarin protects against ischemic injury in vitro and in vivo by decreasing oxidative damage [15], However, it is not clear about the specific mechanism of Scutellarin affects oxidation injury after cerebral ischemia.

Aldose reductase (AR) is a key protein in factor of the polysaccharide pathway of sugar metabolism which regulates the intracellular redox balance as well as maintaining cellular osmotic pressure and oxidative stress [16]. Following AR activation, the body’s antioxidant capacity is reduced by consuming a large amount of reduced coenzyme Ⅱ. It also leads to the accumulation of intracellular sorbitol, which causes increased cell membrane permeability and edema leading to neurological dysfunction [17]. Our previous study showed that the deletion of aldose reductase leads to protection against cerebral ischemic injury indicating its involvement of AR in oxidative stress associated with brain ischemia [18]. Therefore, we consider whether the antioxidant effect of Scutellarin on cerebral ischemia injury is related to the regulation of AR.

Therefore, in these experiments, we first investigate the effect of Scutellarin on tMCAO induced neurological function deficits and brain infarct size in WT and AR-/- mice, then we study the effects of Scutellarin on AR and its downstream gene under cerebral ischemia by quantitative proteomic analysis and proteomic verification molecular biology methods.

Materials And Methods

Experimental animals

One hundred C57BL/6N male mice, SPF grade, weighing 20–24 g and aged between 8–12 weeks were purchased from the Guangdong Medical Experimental Animal Center. The mice were then bred at the Experimental Animal Center of Guangdong Traditional Chinese Medicine Hospital. The aldose reductase knockout ($AR^{-/-}$) mice were obtained from Dr. Sookja Kim Chung, University of Hong Kong [18, 19] and were back-crossed to the 11th generation (N11) strain considered to be congenic with C57BL/6N mice.

One hundred male SPF-grade $AR^{-/-}$ mice weighing 20–24 g and aged 8–12 weeks were selected from this pool. Age-matched normal C57BL/6N mice were, therefore, used as control wild-type mice. All mice were kept at the Experimental Animal Center of Guangzhou University of Chinese Medicine. They were kept at a temperature of (22 ± 2) ° C, a relative humidity of (45 ± 5 %, and a light duration of 12 hours. The mice were housed in cages containing 5 animals and allowed to feed and drink freely.

Transient middle cerebral artery occlusion (tMCAO) model

The tMCAO model was established as previously described [15, 20], except type of anesthesia. Briefly, all mice were individually anesthetized with pentobarbital (50mg/kg, i.p.). Then under the microscope (S100 / OPMI pico, Zeiss, Germany), the right common carotid artery, the right external carotid artery, and the right internal carotid artery were separated, and a 6 − 0 suture (cat: FHX60, Beijing Xinong Technology Co., Ltd.) was attached to the origin and distal end of the right external carotid artery. The special thread plug (cat: A4-162050, Beijing Xinong Technology Co., Ltd.) was introduced into the right external carotid artery and pushed up into the right internal carotid artery until resistance is felt (about 9–10 mm from the carotid bifurcation), blocking the middle cerebral artery. Regional cerebral blood flow was monitored during the whole surgical procedure to confirm appropriate suture placement. The plug was left inserted for 60 min, then the plug was removed. The right external carotid artery was permanently ligated. Mice in the sham group only exposed the arteries without embolization.

Experimental group and Scutellarin administration

All WT and $AR^{-/-}$ mice, 10 in each group, were randomly divided into Sham group, tMCAO + vehicle (0.9% saline) group, Scutellarin low dose group (50mg / kg) and Scutellarin high dose group (100mg/kg). Scutellarin (cat: 27740-01-8, Chengdu Munster Biotechnology Co., Ltd.) was all prepared with 0.9% physiological saline, and the intraperitoneal injection given 2 h before the tMCAO surgery and then 12 h, 24 h, 36 h, 48 h, 60h and 72 h after surgery according to our previous study [15]. The sham operation group and the tMCAO + vehicle group were given the same volume of normal saline at the same times.

Neurological score

After the last administration, the neurological deficits of the mice in each group were evaluated according to the modified Longa score method [21]. Scoring standard: 0: normal limb movements, no neurological deficits; 1: points: when the tail is lifted vertically, the left forepaw is flexed and cannot be straightened; 2: points: the rat leans to the left when walking flat can be rotated to the left; 3 points: unstable walking, the entire body dumped to the left; 4 points: conscious disturbance or unable to walk autonomously. Based on the results of the first neurological impairment score, tMCAO model animals with death, dyspnea, unstable vital signs, or intracranial hemorrhage after execution were discarded.

2,3,5-triphenyltetrazolium chloride (TTC) staining

After neurological scoring, the mice were anesthetized with 10% chloral hydrate by intraperitoneal injection and then brain was perfused with normal saline. The brain was quickly removed into icy water, and then cut into 5 consecutive coronal slices with a thickness of 2 mm. The slices were incubated in 2 %

TTC (cat: T8877, Sigma, USA) for 15 min at 37°C (The infarcted area was white after TTC staining, while the non-infarcted area remained red). The infarct area was calculated using Image J software after taking pictures with a digital camera. Infarct area were presented as the percentage of infarct area of the contralateral hemisphere as previously described [15, 20].

Hematoxylin-eosin (HE) staining

The brain tissue from mice in each group was randomly placed in 4 % paraformaldehyde (cat: JX0100, Guangzhou Jingxin Biological Technology Co., Ltd.) and fixed at room temperature for 24 h. Conventional tissues were dehydrated, wax-impregnated, and paraffin-embedded to make coronal sections (thickness: 4 μm). Each paraffin section was placed in a full-automatic dyeing machine, dewaxed with xylene, rehydrated with alcohol, dyed with hematoxylin, rinsed with distilled water, fixed with alcohol, counterstained with eosin, cleared with xylene, and placed in a microscope after neutral gum seal. The histopathological changes of the penumbra zone in the cortex of each group of mice were assessed, and the morphological structure of neurons in the 200-fold visual field was observed under microcopy (Zeiss, Oberkochen, Germany).

Enzyme-linked immunosorbent assay (ELISA) detection of oxidative stress

Brain tissues were accurately weighed, then added to ice-cold saline saline at a ratio of 1: 9 by weight and then homogenize in an ice bath. The tissue was then centrifuged at 10,000 g for 15 min at 4°C to obtain the supernatant. The following ELISA kits were used oxidative stress across treatment groups: ROS (Lot: 07/2019, Nanjing Herbal Source Biotechnology Co., Ltd.), 4-hydroxynonenal (4-HNE, Lot: UK92FFJBWN, Wuhan Elite Biotech Co., Ltd.), 8-hydroxydeoxyguanosine (8-OHDG, Lot: C22013999, Wuhan Huamei Biological Engineering Co., Ltd.), Neurotrophin-3 (NT-3, Lot: 820013980, Wuhan Huamei Biological Engineering Co., Ltd.), poly ADP-ribose polymerase-1 (PARP1, Lot: 07/2019, Nanjing Herbal Source Biotechnology Co., Ltd.) and 3-nitrotyrosine (3-NT, Lot: 07/2019, Nanjing Herbal Source Biotechnology Co., Ltd.) .

Quantitative Real-time polymerase chain reaction (qRT-PCR) detection of AR, NOX1, NOX2 and NOX4 mRNA in brain tissue

The pooled respective groups' brain tissue from both sides were added to respective 1 ml tubes of trizol (Lot: 191012, Invitrogen, USA) and homogenized in an ice bath. The homogenate was centrifuged at 12,000 g for 10 min at 4 ° C to obtain the supernatant. After the RNA was separated, precipitated and washed with chloroform, isopropanol, and ethanol sequentially, 50 μl of RNase-free ddH_2O was added after drying to fully dissolve the RNA. The RNA concentration was measured by spectrophotometry and the dissolved total RNA stored at -80°C. Following the instruction contained in the Prime Script™ RT reagent Kit (Cat: RR037A, Dalian TaKaRa Biological Technology Co., Ltd.) kit manual, reverse transcription was performed on a PCR instrument to synthesize cDNA from total RNA. cDNA was stored at -20°C until use. Following the kit manual of SYBR PremixEx Taq ^{TM} II (Tli RNaseH Plus) kit (Cat: RR820A, Dalian

TaKaRa Biological Technology Co., Ltd.), Real-time PCR was performed to using the reverse transcription product as a template to detect and quantify AR, NOX1, NOX2 and NOX4 mRNA levels. The primer sequences used for qPCR are listed in Table 1 (Shanghai British Weijieji Trading Co., Ltd). The reaction conditions were as follow: pre-denaturation at 95 ℃ for 10 min, cycle once; denaturation at 95 ℃ for 15 s, 40 cycles; annealing at 65 ℃ for 60 s, extension at 72 ℃ for 60 s, 40 cycles. The mRNA expression level was calculated by the $2^{-\Delta\Delta Ct}$ method. The value for mRNA on the contralateral side served as normal control and was set at 100%.

Table 1
Primer sequence

Name	Primer sequences (5′-3′)	Product length (bp)
AR	Forward primer **5′-**AGAGCATGGTGAAAGGAGCC**-3′**	142
	Reverse primer **5′-**GGTATCACGTTCCCTGAGGC**-3′**	
NOX1	Forward primer **5′-**GTTTCTCTCCCGAAGGACCTC**-3′**	136
	Reverse primer **5′-**TTCAGCCCCAACCAGGAAAC**-3′**	
NOX2	Forward primer **5′-**TGGCGATCTCAGCAAAAGGT**-3′**	131
	Reverse primer **5′-**ACCTTGGGGCACTTGACAAA**-3′**	
NOX4	Forward primer **5′-**ACCAAATGTTGGGCGATTGTG**-3′**	70
	Reverse primer **5′-**GATGAGGCTGCAGTTGAGGT**-3′**	
β-actin	Forward primer **5′-**ACACTCTCCCAGAAGGAGGG**-3′**	147
	Reverse primer **5′-**TTTATAGGACGCCACAGCGG**-3′**	
Note: AR, aldose reductase; NOX, NADPH oxidase.		

Western blot (WB) detection of AR, NOX1, NOX2 and NOX4 protein in brain tissue

The brain tissue was accurately weighed and placed on an ice bath and mixed with a protease inhibitor-containing lysis buffer (cat: P0013, Shanghai Biyuntian Biological Technology Co., Ltd.), and then centrifuged at 12000g at 12°C for at 15 min. The protein concentration of the supernatant was determined by the BCA method. The sample buffer was added to the sample and boiled for 10 min. Load 50 μg of protein was then loaded onto the 10% SDS-PAGE, and run at 80 V for 20 min. The voltage was adjusted to 110 V until the end of the electrophoresis. The membrane was wet transferred for 120 min. Blocking in BSA was carried out for 1 h after which the membrane was placed into the the following primary antibodies: AR (cat: ab175394, abcam, USA); NOX1 (cat: ab55831, abcam, USA); NOX2 (cat: ab80508, abcam, USA); NOX4 (cat: ab154244, abcam, USA) and GAPDH (cat: #5174S, Cell Signaling Technology, USA) and incubated at 4°C overnight (dilution ratios were all 1: 1000). After the overnight incubation, the membranes were washed with TBST and further incubated for 1 h at room temperature

with an HRP-conjugated secondary antibody (1: 3000, cat: #5174S, Cell Signaling Technology, USA) After an hour the strips were washed again, thrice with TBST and then drenched in the ECL chemiluminescence solution to develop color. Detection was carried out in the chemiluminescence system (ChemiDoc XRS, Bio-Rad, PA, USA). Quantitative analysis of protein bands was carried out using Image J software (National Institutes of Health, Bethesda, USA). All experiments were performed in triplicate.

Double Immunofluorescence labeling of AR, NOX1, NOX2, NOX4 and NeuN in brain tissue

Paraffin brain sections were routinely dewaxed in ethanol and water. After washing and soaking in PBS, the working solution in normal goat serum was added dropwise and placed in a 37 ° C incubator for 30 minutes. The overlying serum blocking solution was shaken off, and then AR (cat: ab175394, abcam, USA), NOX1 (cat: ab55831, abcam, USA), NOX2 (cat: NBP2-41291, Novus Biologicals, LLC, USA), NOX4 (cat: ab154244, abcam, USA) and NeuN (cat: ab104224, abcam, USA) primary antibodies (dilution ratios were all 1: 200) were added dropwise to cover the tissues, and incubated overnight at 4°C. The following day, the brain sections were washed 3 times with PBS for 5 min each. Then, the goat anti-rabbit fluorescent secondary antibody (cat: #4412S, CST, USA) and the goat anti-mouse fluorescent secondary antibody (cat: #4409S, CST, USA,dilution ratios were all 1: 2000) were added and incubated for an hour at room temperature in the dark. After washing with PBS, the slices were mounted with anti-fluorescence quencher (cat: P0126, Shanghai Biyuntian Biological Technology Co., Ltd.) and observe under a fluorescence microscope (Zeiss, Oberkochen, Germany). Later, quantitative analysis was performed using Image J software (National Institutes of Health, Bethesda, USA).

Quantitative proteomics profiling detection in AR-/- and WT mice suffered from cerebral ischemia/reperfusion injury

Our previous study showed that the deletion of aldose reductase leads to protection against cerebral ischemic injury indicating its involvement of AR in oxidative stress associated with brain ischemia [16], but the In order to better explore the difference of protein expression between $AR^{-/-}$ and WT mice under cerebral ischemia conditions, quantitative proteomics profiling using quantitative nano-HPLC-MS/MS were performed to compare the protein expression difference between $AR^{-/-}$ and WT mice with or without tMCAO injury at 3d. Brifely, the fresh brain tissue on the right side of the two mice were selected, and each group is represented by 3 biological replicates. Lysis buffer (1% SDS, 8 M urea, 1x Protease Inhibitor Cocktail (Roche Ltd. Basel, Switzerland)) was added into the samples, the samples were then lysed on ice for 30 min and centrifuged at 15000 rpm for 15min at 4℃. The supernatant was collected. Then protein digestion at 37℃ overnight. The peptide mixture was quantified by Pierce™ Quantitative Colorimetric Peptide Assay (23275). The mass spectrometer was run under data independent acquisition mode, and automatically switched between MS and MS/MS mode. The parameters was: (1) MS: scan range (m/z) = 350–1500; resolution = 120,000; AGC target = 4e5; maximum injection time = 50 ms; (2) HCD-MS/MS: resolution = 30,000; AGC target = 1e5; collision energy = 33; (3) DIA (Data independent acquisition) was performed with variable Isolation window, and each window overlapped 1 m/z, and the window number

was 47. The iRT kit (Ki3002, Biognosys AG, Switzerland) was added to all of the samples to calibrate the retention time of extracted peptide peaks. DIA dataset was performed by Spectronaut 13 (Biognosys AG, Switzerland) including data normalization and relative protein quantification. After Welch's ANOVA Test, different expressed proteins were filtered if their p value < 0.05 and fold change > 1.3.

Statistical analysis

SPSS 17.0 statistical software (SPSS Inc. Chicago, IL, USA) was used for statistical analysis. Measurement data were expressed as mean ± standard deviation. One-way ANOVA was used for comparison between multiple groups, and t test was used for comparison between two groups. P < 0.05 was considered statistically significant.

Results

Scutellarin alleviated tMCAO induced neurological function deficits and brain infarct size in mice

According to the time point of administration of Scutellarin explored in our previous study[22],all C57BL/6N male mice subjected to 1 h occlusion followed by 3 days reperfusion (sham controls were not). Neural function scores were assessed according to the Longa score method while the brain tissue sections of each group of mice were evaluated after TTC staining for the computation of cerebral infarct area sizes.

Neurological function deficit scores are shown in Tables 2 and 3. The higher the score, the more severe the cerebral ischemia-reperfusion injury in mice. The data shows higher neurological function deficit scores in the tMCAO model groups compared with the sham group in WT mice. The neurological function deficit scores were significantly decreased by treatment with 100 mg/kg of Scutellarin in WT mice. The high dose of 100mg/kg Scutellarin resulted in a significantly more pronounced preservation of neurological function.

Table 2
Scutellarin alleviated tMCAO induced neurological function deficits in mice

Groups	n	Neurological score					Median ± standard deviation
		0	1	2	3	4	
WT Sham	10	10	0	0	0	0	0.00 ± 0.00###
WT Model	10	1	1	1	6	1	2.50 ± 1.18***
WT Scu 50mg/kg	10	2	2	2	4	0	1.80 ± 1.23***
WT Scu 100mg/kg	10	2	1	6	1	0	1.60 ± 0.97**#
Note: **P < 0.01, ***P < 0.001 vs WT Sham; #P < 0.05, ###P < 0.001 vs WT Model.							

Table 3
Neurological scores of mice in each group

Groups	n	Neurological score					Median ± standard deviation
		0	1	2	3	4	
$AR^{-/-}$ Sham	10	10	0	0	0	0	0.00 ± 0.00###
$AR^{-/-}$ Model	10	1	2	3	4	0	2.00 ± 1.05***
$AR^{-/-}$ Scu 50mg/kg	10	1	2	5	2	0	1.80 ± 0.92***
$AR^{-/-}$ Scu 100mg/kg	10	1	4	4	1	0	1.50 ± 0.85***
Note: ***P < 0.001 vs $AR^{-/-}$ Sham; ###P < 0.001 vs $AR^{-/-}$ Model.							

Representative TTC-staining slices shown in Fig. 1A indicate that the sham-operated mice did not display any infarct. However, there were significantly larger infarct areas in ipsilateral side brain slices of WT mice brains as seen at 3 days after the tMCAO injury. Also, the ipsilateral infarct area sizes were significantly reduced after scutellarin treatment at doses of 50 mg/kg or 100 mg/kg in WT mice. The results also showed that a high dose of 100 mg/kg Scutellarin was more effective in reducing the size of the infarcts. Taken together, these results show that Scutellarin treatment could reduce cerebral infarction area and neurological function deficits after tMCAO injury, which were insistent with our previous findings in cerebral ischemic injury induced rat model [15].

Scutellarin decreased neuronal damage induced by tMCAO

Histological evaluation by hematoxylin and eosin staining was conducted to identify neuronal cell loss in the ischemic cortical border zone (Fig. 1B). The results showed that in WT mice, there was a high number of neurons with a complete structure in the sham group compared with tMCAO model groups. The nuclei of these cells in the sham operated mice are round and large with minimal pyknosis while those in the tMCAO model groups were disordered, swollen with a large number of nuclei either contracted or disappeared. Also, the number of deeply stained neuronal cells as well as the number of vacuolated cells increased at 3d after tMCAO injury. However, 50mg/kg and 100mg/kg Scutellarin could partially prevented neuronal cell loss damage induced by tMCAO in WT mice. These results indicate that Scutellarin could alleviate neuronal injury after ischemia/reperfusion insults in WT mice.

Scutellarin reduces tMCAO induced oxidative damage related ROS, 4-HNE, 8-OHDG, NT-3, PARP1 and 3-NT levels

The following oxidative damage related markers were assessed by ELISA: ROS, 4-HNE, 8-OHDG, NT-3, PARP1 and 3-NT expression. The present data showed that compared with the sham group, the contents of ROS, 4-HNE, 8-OHDG, NT-3, PARP1 and 3-NT in the reperfusion injury model groups increased significantly as seen at 3 days post injury (P < 0.01). Meanwhile, the levels of ROS, 4-HNE, 8-OHDG, NT-3,

PARP1 and 3-NT in the Scutellarin treatment group were significantly reduced than that in saline treated tMCAO model group ($P < 0.01$). Moreover, the concentrations of these indicators were significantly lower in the 100 mg/kg Scutellarin group relative to those in the half dose group ($P < 0.05$). (Fig. 1C)

Collectively, these above results indicate that Scutellarin could reduce the size of the infarct, improve the neurological symptoms, alleviate neuronal injury and decrease oxidative damage induced by cerebral ischemia in mice. Thus, Scutellarin could be an effective anti-oxidative injury agent for treating cerebral ischemia.

Scutellarin down-regulated tMCAO induced AR mRNA and protein level

Our previous study showed that the deletion of aldose reductase leads to protection against cerebral ischemic injury indicating its involvement of AR in oxidative stress associated with brain ischemia [16], so whether the antioxidant effect of Scutellarin on cerebral ischemia injury is related to AR gene. Both qPCR and Western-blot analysis were used to check the mRNA and protein expression levels of AR gene in the ipsilateral side of brain at 3 days after tMCAO. The results showed that AR mRNA and protein expression were all significantly increased in the tMCAO model group compared to that in the sham group in WT mice at 3 days after ischemic injury; Moreover, the levels of AR mRNA and protein were decreased by Scutellarin treatment and the expression levels recorded in the 100 mg/kg Scutellarin treatment group were significantly lower than in the 50 mg/kg Scutellarin treatment group ($P < 0.01$, Fig. 2A and 2B). These results showed that Scutellarin could down-regulated tMCAO induced AR mRNA and protein levels in a dose dependent manner.

The therapeutic effect of Scutellarin on the reduction of cerebral infarction area and neurological function deficits were abolished in AR-/- mice under ischemia cerebral injury

All $AR^{-/-}$ mice subjected to 1 h occlusion followed by 3 days reperfusion (sham controls were not). Neural function scores were assessed according to the Longa score method while the brain tissue sections of each group of mice were evaluated after TTC staining for the computation of cerebral infarct area sizes.

Neurological function deficit scores are shown in Table 3. The result showed that higher neurological function deficit scores in the tMCAO model groups compared with the sham group in $AR^{-/-}$ mice, but the neurological function deficit scores were no significantly difference by treatment with 50 mg/kg or 100 mg/kg of Scutellarin compared with that in tMCAO model group in $AR^{-/-}$ mice. Representative TTC-staining slices shown in Fig. 3 indicate that in the $AR^{-/-}$ mice, the sham-operated mice did not display any infarct. However, there were significantly larger infarct areas in ipsilateral side brain slices of $AR^{-/-}$ mice brains as seen at 3 days after the tMCAO injury. But the ipsilateral infarct area sizes were not significantly difference after scutellarin treatment at doses of 50 mg/kg or 100 mg/kg in $AR^{-/-}$ mice. The results indicated that Scutellarin treatment had abolished the effects on the reduction of cerebral infarction area and neurological function deficits when AR gene knockout after tMCAO injury. The above results suggested that the antioxidative effect of Scutellarin on cerebral ischemia injury related to AR regulation.

Comprehensive Proteome Profiles of Brains in AR-/- and WT mice after cerebral ischemia injury

Our previous study showed that its involvement of AR in oxidative stress associated with cerebral ischemia [18], but the protein target of AR in cerebral ischemia is not clear. To better explore the molecular mechanisms and discover the potential targets of AR in tMCAO injury, a data independent acquisition (DIA) quantitative proteomic analysis was performed on cerebral ischemic brain tissues in WT and $AR^{-/-}$ mice at 3d after tMCAO injury using the nano-HPLC-MS/MS Analysis approach in the current study. Different expressed proteins (DEPs) were filtered if their p value < 0.05 and fold change > 1.3. In total, 123 DEPs were detected to be specific-differentially expressed in sham controls compared with tMCAO group in WT mice, of which 61 and 62 were significantly up- and downregulated, respectively, 770 DEPs in tMCAO group of $AR^{-/-}$ mice compared with in tMCAO group of WT mice, with 350 and 420 representing up- and down-regulation, whereas 704 DEPs were detected to be specific-differentially expressed in sham group of $AR^{-/-}$ mice compared with in Sham group of WT mice, of which 331 and 373 were significantly up- and downregulated, respectively. The protein expression patterns and DEPs were visualized via volcano plots in Fig. 4A,4B and 4C. Hierarchical clustering shows that the samples cluster in agreement with the group information in additional files Fig. S1. Furthermore, the Venn diagram analysis revealed that 62 DEPs were co-expressed between WT tMCAO versus WT sham and $AR^{-/-}$ tMCAO versus WT tMCAO but there is 21 DEPs among these 62 DEPs were also co-expressed between WT Sham versus $AR^{-/-}$ sham in Fig. 4D.

Go enrichment and KEGG pathway enrichment in AR-/- and WT mice after cerebral ischemia injury

To get a deep overview of molecular and functional differences of DEPs after cerebral ischemia with or without AR gene, GO enrichment and KEGG pathway annotation were carried out. GO terms of BP, cell component (CC), and MF in WT tMCAO versus WT sham and $AR^{-/-}$ tMCAO versus WT tMCAO are summarized in additional files Table S1 and S2 and every term was constructed with P-values less than 0.05, as shown in additional files Figure S2, after GO categorical analysis.

When the WT mice were subjected to the I/R injury induced by tMCAO, the BP analysis demonstrated that the majority of DEPs (additional files Fig S3B) were significantly involved in the catabolic process ($P = 1.37 \times 10^{-6}$), organic substance catabolic process ($P = 3.20 \times 10^{-6}$), cellular catabolic process ($P = 1.09 \times 10^{-6}$), and so forth. Regarding the CC, most DEPs (additional files Fig S3B) predominately originated from the intracellular part ($P = 1.07 \times 10^{-2}$), cytoplasmic part ($P = 2.64 \times 10^{-5}$), intracellular organelle ($P = 4.98\times 10^{-3}$), and so forth. The representative MF of DEPs (additional files Fig S3B) were mainly classified into identical protein binding ($P = 7.79 \times 10^{-4}$), calcium ion binding ($P = 7.55 \times 10^{-4}$), microtubule binding ($P = 5.16 \times 10^{-3}$), and so forth. These results demonstrated that the molecular mechanisms of I/R induced by tMCAO were complex, and many BPs such as protein kinase activity, autophagy, cytokine

production involved in inflammatory response and cell proliferation participated in this physiopathologic procedure which required different MF of DEPs and cell organelles.

When AR gene knockout under cerebral ischemia condition, compared with $AR^{-/-}$ tMCAO and WT tMCAO group, the BP of DEPs (additional files Fig S3A) were strongly enriched in response to purine ribonucleotide biosynthetic process ($P = 4.39 \times 10^{-7}$), ribonucleotide biosynthetic process ($P = 4.7 \times 10^{-7}$), oxidoreduction coenzyme metabolic process ($P = 4.23 \times 10^{-7}$) and so forth. The DEPs in CC (additional files Fig S3A) mainly participated in cytosol ($P = 3.96 \times 10^{-6}$), mitochondrial part ($P = 1.84 \times 10^{-6}$), membrane protein complex ($P = 3.07 \times 10^{-6}$), and so forth. The DEPs clustered in MF (additional files Fig S3A) primarily associated with catalytic activity ($P = 5.34 \times 10^{-6}$), ion binding ($P = 1.05 \times 10^{-5}$), anion binding ($P = 3.44 \times 10^{-6}$), and so forth.

As we known, AR is a key enzyme in the polyol pathway, catalyzes nicotinamide adenosine dinucleotide phosphate-dependent reduction of glucose to sorbitol, leading to excessive accumulation of intracellular reactive oxygen species (ROS) in various tissues of diabetes mellitus including the heart, vasculature, neurons, eyes, and kidneys [16], so we focus on the abnormal cellular responses especially in oxidoreduction activity after I/R injury under AR knockout condition, possibly which was the underlying mechanism in protection of I/R. What attracts our great attention and interest of Go enrichment is that AR knockout in cerebral ischemia affects oxidoreduction activity acting on NADPH.

In addition, the dysregulated DEPs in WT tMCAO versus WT sham and $AR^{-/-}$ tMCAO versus WT tMCAO were mainly mapped into the following pathways summarized in additional files Table S3 and S4, and presented in bar plots versus P-values and listed in additional files Fig. S3. The KEGG pathway analysis of DEPs (additional files Fig. S3) in WT tMCAO versus WT sham was mainly related with cell adhesion molecules (4.79×10^{-3}), endocytosis (4.63×10^{-2}), focal adhesion (1.29×10^{-2}), and so forth. Interestingly, the DEPs in $AR^{-/-}$ tMCAO versus WT tMCAO (additional files Fig. S3) were mainly associated with metabolic pathways (8.69×10^{-22}), oxidative phosphorylation (1.12×10^{-12}), Parkinson's disease (3.31×10^{-11}) and so forth. According to the KEGG pathway enrichment analysis, it was evident that AR maybe plays an important role in activating anti-oxidative related pathway which responsible for I/R injury, which was consistent with GO analysis.

AR knockout decreased tMCAO induced NOX isoforms mRNA and protein in mouse brain.

Since AR knockout in cerebral ischemia affects oxidoreduction activity acting on NADPH from the above proteomics analysis. Our previous study showed that Scutellarin protects against ischemic injury in vitro and in vivo by downregulating NOX2 derived reactive oxygen species (ROS) induced oxidative damage in rats. In the brain there are NOX1, 2 and 4 isoforms of NADPH oxidases. Previous studies have shown that NOX1 and NOX4 participate in ROS-induced neuronal apoptosis and brain injury during ischemia-reperfusion in rats [23–24]. So NOX1, NOX2 and NOX4 were chosen for further validation to explore whether AR regulate NOX isoforms under I/ R injury by qPCR, western blotting and double Immunofluorescence labeling in WT and $AR^{-/-}$ mice after cerebral ischemia injury. At 3 days after tMCAO

injury, the results of qPCR and western blot showed that there were increased NOX1, NOX2 and NOX4 mRNA and protein expressions in both the WT and $AR^{-/-}$ tMCAO injured mice. The expression of NOX1, NOX2 and NOX4 at mRNA and protein levels in $AR^{-/-}$ mice was less than that in WT mice among the sham group. Moreover, NOX1, NOX2 and NOX4 mRNA and protein were significantly lower in the $AR^{-/-}$ tMCAO model group compared to the WT tMCAO model group. Our data indicated that AR knockout resulted in a significant decrease in the protein expression of NOX at 3d after tMCAO injury (Fig. 5).

To furtherly check the expression of AR and NOX isoforms in neurons in the penumbra regions of the ipsilateral side of brain after tMCAO injury, immunofluorescence staining of AR, NOX1, NOX2 and NOX4 with neuronal nuclei (NeuN) was carried out on brain sections harvested after 3 days of reperfusion. Immunostaining evidence indicates that NeuN is distributed in the nuclei of mature neurons in nearly all parts of vertebrate nervous system, nearly all nuclei and perikaryons and some proximal processes are strongly positive for NeuN expression. AR, NOX1, NOX2 and NOX4 were all expressed in cytoplasm of brain cells. The results showed that the density and distribution of the AR, NOX1, NOX2 and NOX4 co-staining NeuN positive immunoreactions showed increases in the ipsilateral side brain in tMCAO model groups, while fewer AR, NOX1, NOX2 and NOX4 co-staining NeuN positive cells were observed in the sham group both in WT and $AR^{-/-}$ tMCAO mice. Moreover, there were less NOX1, NOX2 and NOX4 co-staining NeuN positive cells were significantly lower in the ipsilateral side of brain of $AR^{-/-}$ tMCAO model group compared to the WT tMCAO model group, which is consistent with the results of Western-blot analysis (Fig. 6).The observations suggest that AR could regulate the level of NOX1,NOX2, NOX4 mRNA and protein in neurons efficiently after tMCAO injury and that it may be acting upstream of NOX isoforms following cerebral ischemia.

Scutellarin down-regulated tMCAO induced NOX isoforms mRNA and protein level

Both qPCR and Western-blot analysis were used to check the mRNA and protein expression levels of NOX1, NOX2 and NOX4 gene in the ipsilateral side of brain at 3 days after tMCAO. The results showed that NOX1, NOX2, and NOX4 mRNA and protein expression were all significantly increased in the tMCAO model group compared to that in the sham group in WT mice at 3 days after ischemic injury; Moreover, the levels of NOX1, NOX2, and NOX4 mRNA and protein were decreased by Scutellarin treatment and the expression levels recorded in the 100 mg/kg Scutellarin treatment group were significantly lower than in the 50 mg/kg Scutellarin treatment group ($P < 0.01$, Fig. 2A and 2B). These results showed that Scutellarin could down-regulated tMCAO induced NOX isoforms mRNA and protein levels in a dose dependent manner. The above results suggested that Scutellarin treatment could reduce ischemic brain injury in tMCAO injury mice and would acts on the AR-NOX Axis to remediate oxidative stress injury in a mouse model of cerebral ischemia/reperfusion injury.

Discussion

Our previous study indicated that AR involvement in oxidative stress associated with cerebral ischemia and AR knockout leads to protection against cerebral ischemic injury [18], but the protein target of AR in cerebral ischemia is not clear. AR is a key protein in factor of the polysaccharide pathway of sugar metabolism which regulates the intracellular redox balance as well as maintaining cellular osmotic pressure and oxidative stress [16]. AR also plays an important role in the induction of hyperglycemia-induced oxidative stress whereby excessive amounts of glucose are shunted into the polyol pathway. Here, AR reduces glucose into sorbitol at the expense of NADPH. Since NADPH is essential for generation of glutathione (GSH) (intracellular antioxidant) from oxidized glutathione disulfide (GSSG), the depletion of NADPH by the AR pathway may impair intracellular antioxidant defense. Sorbitol is then converted to fructose by succinate dehydrogenase (SDH) (along with the production of NADH) ultimately causing liberation of ROS via NOX signaling [25] Taken together, these findings suggest that there is a relationship between AR and NOX signaling. Some studies have reported that regulating the activity of AR and NOX can reduce platelet aggregation and apoptosis under high glucose condition [26, 27]. Various animal studies of cerebral ischemia by others and in our previous study note that both AR and NOX isoforms genes are induced in the brain. However, whether there is a regulatory relationship between these two genes after cerebral ischemia is unclear. In this study, we performed quantitative proteomics profiling using quantitative nano-HPLC-MS/MS to compare the protein expression difference between $AR^{-/-}$ and WT, and the result showed that AR knockout in cerebral ischemia affects oxidoreduction activity acting on NADPH. Nicotinamide adenine dinucleotide phosphate oxidase (NOX)derived reactive oxygen species (ROS) serve an important role in the evolution of cerebral ischemia/reperfusion (I/R) injury [28]. In the brain there are NOX1, 2 and 4 isoforms. Previous studies have shown that NOX2 and NOX4 participate in ROS-induced neuronal apoptosis and brain injury during ischemia-reperfusion in rats [29]. It has also been reported that targeting NOX4, a source of oxidative stress, is neuroprotective after ischemic stroke [23]. NOX1 signaling contributes to oxidative damage to DNA and subsequent cortical neuronal degeneration as well as functional recovery, and regulation of ischemic neurogenesis in the peri-infarct regions after stroke [24].Our previous study also found that NOX2 expression were significantly increased the oxygen–glucose-deprivation/reperfusion (OGD/R) exposed astrocytes and those on the ipsilateral side of ischemic brain [15]. So which and how NOX is regulated by AR under cerebral ischemia injury has not yet been fully elucidated. Then we furtherly check the AR and NOX isoforms expression in the in $AR^{-/-}$ and WT suffered from tMCAO mouse model. Our results showed that there was a significant decrease in the protein expression of NOX isoforms after 72 h of tMCAO injury in $AR^{-/-}$ mice. This indicated that AR regulated NOX isoforms expression under ischemia stroke conditions. Our previous study found that Scutellarin protects against ischemic injury *in vitro* and *in vivo* by downregulating NOX2 derived reactive oxygen species induced oxidative damage [15]. This study further demonstrated that Scutellarin does not only down-regulate the expression of NOX2, but it also reduced other NOX isoforms such as NOX1 and NOX4 as well as associated oxidative injury markers after cerebral ischemia. Most importantly, and Scutellarin also could down-regulated the expression of the AR gene. As a result, we think that the protective effects of Scutellarin on ischemic stroke is through the AR-NOX axis to modulate the oxidative stress injury.(Fig. 7)

Cerebral ischemia-reperfusion injury involves complex and diverse mechanisms [32]. Enhanced oxidative stress characterized by increased expression of oxygen free radicals is one of its main pathological mechanisms [33, 34]. After cerebral ischemia occurs, prompt blood flow can effectively reduce brain tissue damage and associated neurological dysfunction [35]. However, during reperfusion a large amount of ROS such as superoxide free radicals, hydroxyl free radicals, and excessive increased hydrogen oxide are generated and can cause deoxyribonucleotide (DNA) damage, protein and lipid oxidation, and eventually cause or exacerbate neuronal damage [36]. ROS easily affect lipids on cell membranes and lipid peroxidation produces a large number of lipid peroxides (toxic aldehydes such as 4-HNE) which increases cell membrane permeability as well as disrupt their structural integrity and functions [37]. In addition, 8-OHDG can activate hydroxyl radicals or oxygen free radicals to further damage the mitochondria in neurons resulting in neuronal energy utilization disorders [38]. In the case of ischemia-reperfusion, due to the production of a large number of free radicals and oxidants, PARP1 gets activated causing a large amount of intracellular NAD to be consumed, and eventually ATP gets depleted [39]. Reducing the level of 3-NT in ischemia-reperfusion damaged brain tissue has been shown to attenuate cerebral ischemia-reperfusion injury [40]. Oxidative stress is widely involved in various pathophysiological processes such as aging and inflammation [41]. NT-3 supports the growth and development of neurons, and also participates in the occurrence and development of various inflammatory diseases [42]. The results of the current experiments showed that the oxidative stress-related factors (ROS, 4-HNE, 8-OHDG, PARP1, NT-3 and 3-NT) are expressed in WT mice after tMCAO significantly more than that in the sham operated group. This indicated that the oxidative stress response of the cerebral ischemia-reperfusion model was indeed activated. Therefore, measures aimed at reducing oxidative stress were considered to be of potential value in the treatment of ischemic stroke. Under cerebral ischemia, the source of ROS is also an important scientific question. NOX is a key enzyme in the production of ROS (such as O^{2-} and H_2O_2) after cerebral ischemic injury [43]. Also, NOX activity is among the three distinct processes that generate ROS [44]. AR is also a major contributor to oxidative stress in diabetic neuropathy [45]. A previous study also reported that AR contributes to oxidative stress after ischemic/reperfusions since the expression of platelet aggregation rate (PAR) and nitrotyrosine, indicators of increased oxidative or nitrosative stress, is decreased in $AR^{-/-}$ brains after tMCAO[18]. So the antioxidant drugs with therapeutic effects on cerebral ischemic injury may have multi-target characteristics.

Scutellarin has anti-neurotoxicity, anti-inflammatory response, anti-oxidative stress, and neuroprotective effects [46]. Studies have reported that Scutellarin can inhibit some molecules related to neuronal apoptosis signaling pathways thereby protecting against neural damage caused by cerebral ischemia [47]. ROS produced during ischemia-reperfusion injury has been shown to activate AR [48]. After activation, AR can reduce the body’s antioxidant capacity and aggravate neural dysfunction [49]. A previous study showed that the deletion of aldose reductase leads to protection against cerebral ischemic injury while its inhibition had therapeutic potential against cerebral ischemic injury, demonstrating its involvement in oxidative stress and cerebral ischemic injury [18]. Based on this, it was speculated that Scutellarin may have the effect of regulating AR to prevent oxidative stress. The present experimental results elucidated that when tMCAO injured mice were treated with Scutellarin, tMCAO induced AR

expression was reduced. In addition, the area under cerebral infarction was also reduced. This illuminated the pathological role of AR in tMCAO and also exposed the pharmacotherapeutic effects of Scutellarin. Therefore, AR is one of the targets of Scutellarin for ischemic stroke protection.

Basic research showed that increasing AR expression changed intracellular NADPH/NAD ratio, affected intracellular redox status, increased intracellular ROS production, leading to endothelial cell damage [50]. NADPH was a key protein that catalyzes generation of oxygen free radicals [51]. During ischemia-reperfusion, NOX, a main source of ROS, is activated in the brain tissue thereby generating a large amount of ROS and triggers oxidative stress and associated tissue oxidative damage [52, 53]. The central nervous system expressed NOX1, NOX2, NOX4, indicating that these isoforms participates in oxidative damage of the brain tissue [54–56]. It was, thus, speculated that AR may regulate NOX expression under cerebral ischemia. According to the current results, isoforms NOX1, NOX2, and NOX4 were significantly decreased tMCAO in $AR^{-/-}$ mice suggesting that AR may regulate NOX expression under cerebral ischemia. In WT mice, subjected to tMCAO, AR and NOX1, NOX2, and NOX4 expression were attenuated by Scutellarin treatment. This showed that Scutellarin can inhibit the tMCAO induced overexpression of AR and NOX isoforms. These results suggest that AR is the upstream protein regulating NOX in the Scutellarin medicated neuroprotection against cerebral ischemia. Our previous study found that Scutellarin protects against ischemic injury *in vitro* and *in vivo* by downregulating NOX2, decreasing oxidative damage, and reducing apoptotic cell death [15]. In this study, the results showed that Scutellarin could decrease the neurological deficit and brain infarct area in WT mice, but the effect of Scutellarin abolished in $AR^{-/-}$ mice. This indicated that Scutellarin treatment have effects tMCAO injury would act on AR-NOX Axis to remediate oxidative stress injury in mouse.

Conclusions

Therefore, from the above results, we demonstrated that Scutellarin could play a protective role of cerebral ischemia in mice. Scutellarin acts on the AR-NOX Axis to remediate oxidative stress injury in a mouse model of cerebral ischemia/reperfusion injury.

Abbreviations

Aldose reductase (AR);C57BL/6N mice (Wild-type, WT);AR knockout ($AR^{-/-}$);transient middle cerebral artery occlusion (tMCAO);4-hydroxynonenal (4-HNE);8-hydroxydeoxyguanosine (8-OHDG);Neurotrophin-3 (NT-3);poly ADP-ribose polymerase-1 (PARP1);3-nitrotyrosine (3-NT);Different expressed proteins (DEPs) ;cell component (CC);reactive oxygen species (ROS);neuronal nuclei (NeuN);succinate dehydrogenase (SDH);Nicotinamide adenine dinucleotide phosphate oxidase(NOX);oxygen–glucose-deprivation/reperfusion (OGD/R);platelet aggregation rate (PAR)

Declarations

Competing interests

The authors declare that they have no competing interests.

Funding

This study was financially supported by the National Natural Science Foundation of China, No. 81303115, 81774042, 81771353 and 81904104; the Pearl River S & T Nova Program of Guangzhou, No.201806010025; the Specialty Program of Guangdong Province Hospital of Traditional Chinese Medicine of China, No. YN2016MJ07, 2015KT1294, YN2015MS02, and YN2018ZD07 and the Youth Pilot Project of Chinese Society of Traditional Chinese Medicine, No. CACM-2018-QNRC2-C09; the Natural Science Foundation of Guangdong Province of China, No. S2013040016915; the Science and Technology Program of Guangzhou City of China, No. 201604020003; the Postdoctoral Foundation of China, No. BBK42913K09, 201003345, and BBH429151701; Hong Kong Scholar Program; Guangdong Provincial Key Laboratory of Research on Emergency in TCM, No.2017B030314176; Guangzhou University of TCM 2017 high level University Construction Program, No. A1-AFD018171Z11096 and the Administration of Traditional Chinese Medicine of Guangdong Province, No.20211203.

Disclosure policy

Authors do not have any financial or other disclosures.

Author contributions

M.D, J.S and X.C conceived and designed the experiments. M.D, L.P, S.W, Z.G, X.W, Y.H and Y.C performed the experiments. M.D, Y.H, L.P and X.C analyzed the data. M.D, J.S, X.C wrote the manuscript. M.D, J.S, Y.H, Y.C, L.Z, S.C and X.C provided revision of the paper. All authors read and approved the manuscript.

Acknowledgments

We express our thanks to Prof.Cheng Xiao at Guangzhou University of Chinese Medicine, for her interest and support.

Availability of data and materials

All materials are available from the corresponding author.

Ethics approval and consent to participate

The Experimental Animal Ethics Committee of Guangdong Provincial Hospital of Traditional Chinese Medicine approved this study (No. 2019049).

Consent for publication

Not applicable.

References

[1] Lloyd-Jones D, Adams RJ, Brown TM, Carnethon M, Dai S, De Simone G, et al. American Heart Association Statistics Committee and Stroke Statistics Subcommittee, Heart disease and stroke statistics–2010 update: a report from the American Heart Association. Circulation. 2010;121:46-215.

[2] Kraft P, De Meyer SF, Kleinschnitz C. Next-generation antithrombotics in ischemic stroke: preclinical perspective on 'bleeding-free antithrombosis'. J Cereb Blood Flow Metab. 2012;32:1831-1840.

[3] Vivien D, Gauberti M, Montagne A, Defer G, Touzé E. Impact of tissue plasminogen activator on the neurovaScutellarinlar unit: from clinical data to experimental evidence. J Cereb Blood Flow Metab. 2011;31:2119-2134.

[4] Yellon DM, Hausenloy DJ (2007). Myocardial reperfusion injury. N Engl J Med. 2007;357:1121–1135.

[5] Zille M, Farr TD, Przesdzing I, Müller J, Sommer C, Dirnagl U, et al. Visualizing cell death in experimental focal cerebral ischemia: promises, problems, and perspectives. J Cereb Blood Flow Metab. 2012;32:213-231.

[6] Qin AP, Liu CF, Qin YY, Hong LZ, Xu M, Yang L, et al. Autophagy was activated in injured astrocytes and mildly decreased cell survival following glucose and oxygen deprivation and focal cerebral ischemia. Autophagy. 2010;6:738-753.

[7] Bredesen DE, Rao RV, Mehlen P. Cell death in the nervous system. Nature. 2006;443:796-802.

[8] Enzmann G, Kargaran S, Engelhardt B. Ischemia-reperfusion injury in stroke: impact of the brain barriers and brain immune privilege on neutrophil function. Ther Adv Neurol Disord. 2018;11:1756286418794184.

[9] Mohsenpour H, Pesce M, Patruno A, Bahrami A, Pour PM, Farzaei MH. A Review of Plant Extracts and Plant-Derived Natural Compounds in the Prevention/Treatment of Neonatal Hypoxic-Ischemic Brain Injury. Int J Mol Sci. 2021;22:833.

[10] Mo J, Yang R, Li F, Zhang X, He B, Zhang Y, et al. Scutellarin protects against vascular endothelial dysfunction and prevents atherosclerosis via antioxidation. Phytomedicine. 2018;42:66-74.

[11] Hua F, Peng L, Qiang K, Zhi-Long Z, Ji W, Jia-Yi C. Metabolism and Pharmacological Mechanisms of Active Ingredients in Erigeron breviscapus. Curr Drug Metab. 2020;In press.

[12] Gao L, Tang H, Zeng Q, Tang T, Chen M, Pu P. The anti-insulin resistance effect of scutellarin may be related to antioxidant stress and AMPKα activation in diabetic mice. Obes Res Clin Pract. 2020;14:368-374.

[13] Wu H, Jia L. Scutellarin attenuates hypoxia/reoxygenation injury in hepatocytes by inhibiting apoptosis and oxidative stress through regulating Keap1/Nrf2/ARE signaling. Biosci Rep. 2019;39:BSR20192501.

[14] Hu X, Wu X, Zhao B, Wang Y. Scutellarin protects human retinal pigment epithelial cells against hydrogen peroxide (H 2 O 2)-induced oxidative damage. Cell Biosci. 2019;9:12.

[15] Sun JB, Li Y, Cai YF, Huang Y, Liu S, Yeung PK, et al. Scutellarin protects oxygen/glucose-deprived astrocytes and reduces focal cerebral ischemic injury. Neural Regen Res. 2018;13:1396-1407.

[16] Tang WH, Martin KA, Hwa J. Aldose reductase, oxidative stress, and diabetic mellitus. Front Pharmacol. 2012;3:87.

[17] Hwang YC, Sato S, Tsai JY, Yan S, Bakr S, Zhang H, et al. Aldose reductase activation is a key component of myocardial response to ischemia. FASEB J. 2002;16:243-245.

[18] Lo AC, Cheung AK, Hung VK, Yeung CM, He QY, Chiu JF, et al. Deletion of aldose reductase leads to protection against cerebral ischemic injury. J Cereb Blood Flow Metab. 2007;27:1496-1509.

[19] Ho HT, Chung SK, Law JW, Ko BC, Tam SC, Brooks HL, et al. Aldose reductase-deficient mice develop nephrogenic diabetes insipidus. Mol Cell Biol. 2000;20:5840-5846.

[20] Cheng X, Yeung PKK, Zhong K, Zilundu PLM, Zhou L, Chung SK, et al. Astrocytic endothelin-1 overexpression promotes neural progenitor cells proliferation and differentiation into astrocytes via the Jak2/Stat3 pathway after stroke. J Neuroinflammation. 2019;16:227.

[21] Deng QW, Yang H, Yan FL, Wang H, Xing FL, Zuo L, et al. Blocking Sympathetic Nervous System Reverses Partially Stroke-Induced Immunosuppression but does not Aggravate Functional Outcome After Experimental Stroke in Rats. Neurochem Res. 2016;41:1877-1886.

[22] Sun JB, Li Y, Cai YF, Huang Y, Liu S, Yeung PK, et al. Scutellarin protects oxygen/glucose-deprived astrocytes and reduces focal cerebral ischemic injury, Neural Regen Res. 2018;13:1396-1407.

[23] Radermacher KA, Wingler K, Langhauser F, Altenhöfer S, Kleikers P, Hermans JJ. Neuroprotection after stroke by targeting NOX4 as a source of oxidative stress. Antioxid Redox Signal. 2013;18:1418-1427.

[24] Choi DH, Kim JH, Lee KH, Kim HY, Kim YS, Choi WS, et al. Role of neuronal NADPH oxidase 1 in the peri-infarct regions after stroke. PLoS One. 2015;10:e0116814.

[25] Tang WH, Martin KA, Hwa J. Aldose reductase, oxidative stress, and diabetic mellitus.frontiers in pharmacology. Front Pharmacol. 2012;3:87.

[26] Paul M, Hemshekhar M, Kemparaju K, Girish KS. Berberine mitigates high glucose-potentiated platelet aggregation and apoptosis by modulating aldose reductase and NADPH oxidase activity. Free Radic Biol Med. 2019;130:196-205.

[27] Warren AM, Knudsen ST, Cooper ME. Diabetic nephropathy: an insight into molecular mechanisms and emerging therapies. Expert Opin Ther Targets. 2019;23:579-591.

[28] Yao H, Ago T, Kitazono T, Nabika T. NADPH Oxidase-Related Pathophysiology in Experimental Models of Stroke. Int J Mol Sci. 2017;18:pii:E2123.

[29] Wang J, Liu Y, Shen H, Li H, Wang Z, et al. Nox2 and Nox4 Participate in ROS-Induced Neuronal Apoptosis and Brain Injury During Ischemia-Reperfusion in Rats. Acta Neurochir Suppl. 2020;127:47-54.

[30] Radermacher KA, Wingler K, Langhauser F, Altenhöfer S, Kleikers P, Hermans JJ. Neuroprotection after stroke by targeting NOX4 as a source of oxidative stress. Antioxid Redox Signal. 2013;18:1418-1427.

[31] Choi DH, Kim JH, Lee KH, Kim HY, Kim YS, Choi WS, et al. Role of neuronal NADPH oxidase 1 in the peri-infarct regions after stroke. PLoS One. 2015;10:e0116814.

[32] Stoll G, Nieswandt B. Thrombo-inflammation in acute ischaemic stroke - implications for treatment. Nat Rev Neurol. 2019;15:473-481.

[33] Carbone F, Bonaventura A, Montecucco F. Neutrophil-Related Oxidants Drive Heart and Brain Remodeling After Ischemia/Reperfusion Injury. Front Physiol. 2020;10:1587.

[34] Wang Z, Zhou F, Dou Y, Tian X, Liu C, Li H, et al. Melatonin Alleviates Intracerebral Hemorrhage-Induced Secondary Brain Injury in Rats via Suppressing Apoptosis, Inflammation, Oxidative Stress, DNA Damage, and Mitochondria Injury. Transl Stroke Res. 2018;9:74-91.

[35] Bavarsad K, Barreto GE, Hadjzadeh MA, Sahebkar A. Protective Effects of Curcumin Against Ischemia-Reperfusion Injury in the Nervous System. Mol Neurobiol. 2019;56:1391-1404.

[36] Chen SD, Yang JL, Lin TK, Yang DI. Emerging Roles of Sestrins in Neurodegenerative Diseases: Counteracting Oxidative Stress and Beyond. J Clin Med. 2019;8:pii:E1001.

[37] Guo JJ, Ma LL, Shi HT, Zhu JB, Wu J, Ding ZW, et al. Alginate Oligosaccharide Prevents Acute Doxorubicin Cardiotoxicity by Suppressing Oxidative Stress and Endoplasmic Reticulum-Mediated Apoptosis. Mar Drugs. 2016;14:pii:E231.

[38] Furukawa A, Kawamoto Y, Chiba Y, Takei S, Hasegawa-Ishii S, Kawamura N, et al. Proteomic identification of hippocampal proteins vulnerable to oxidative stress in excitotoxin-induced acute neuronal injury. Neurobiol Dis. 2011;43:706-714.

[39] van Wijk SJ, Hageman GJ. Poly(ADP-ribose) polymerase-1 mediated caspase-independent cell death after ischemia/reperfusion. Free Radic Biol Med. 2005;39:81-90.

[40] Tsoi B, Chen X, Gao C, Wang S, Yuen SC, Yang D, et al. Neuroprotective Effects and Hepatorenal Toxicity of Angong Niuhuang Wan Against Ischemia-Reperfusion Brain Injury in Rats. Front Pharmacol. 2019;10:593.

[41] Yao X, Carlson D, Sun Y, Ma L, Wolf SE, Minei JP, et al. Mitochondrial ROS Induces Cardiac Inflammation via a Pathway through mtDNA Damage in a Pneumonia-Related Sepsis Model. PLoS One. 2015;10:e0139416.

[42] Han Q, Ordaz JD, Liu NK, Richardson Z, Wu W, Xia Y, et al. Descending motor circuitry required for NT-3 mediated locomotor recovery after spinal cord injury in mice. Nat Commun. 2019;10:5815.

[43] Abramov AY, Scorziello A, Duchen MR. Three distinct mechanisms generate oxygen free radicals in neurons and contribute to cell death during anoxia and reoxygenation. J Neurosci. 2007;27:1129-1138.

[44] Kahles T, Luedike P, Endres M, Galla HJ, Steinmetz H, Busse R, et al. NADPH oxidase plays a central role in blood-brain barrier damage in experimental stroke. Stroke. 2007;38:3000-3006.

[45] Ho EC, Lam KS, Chen YS, Yip JC, Arvindakshan M, Yamagishi S, et al. Aldose reductase-deficient mice are protected from delayed motor nerve conduction velocity, increased c-Jun NH2-terminal kinase activation, depletion of reduced glutathione, increased superoxide accumulation, and DNA damage. Diabetes. 2006;55:1946-1953.

[46] Wang L, Ma Q. Clinical benefits and pharmacology of Scutellarintellarin: A comprehensive review. Pharmacol Ther. 2018;190:105-127.

[47] Yuan Y, Fang M, Wu CY, Ling EA. Scutellarin as a Potential Therapeutic Agent for Microglia-Mediated Neuroinflammation in Cerebral Ischemia. Neuromolecular Med. 2016;18:264-273.

[48] Liu KX, Li C, Li YS, Yuan BL, Xu M, Xia Z, et al. Proteomic analysis of intestinal ischemia/reperfusion injury and ischemic preconditioning in rats reveals the protective role of aldose reductase. Proteomics. 2010;10:4463-4475.

[49] Fu J, Tay SS, Ling EA, Dheen ST. Aldose reductase is implicated in high glucose-induced oxidative stress in mouse embryonic neural stem cells. J Neurochem. 2007;103:1654-1665.

[50] Huang Z, Hong Q, Zhang X, Xiao W, Wang L, Cui S, et al. Aldose reductase mediates endothelial cell dysfunction induced by high uric acid concentrations. Cell Commun Signal. 2017;15:3.

[51] Kalinina S, Breymayer J, Reeß K, Lilge L, Mandel A, Rück A, et al. Correlation of intracellular oxygen and cell metabolism by simultaneous PLIM of phosphorescent TLD1433 and FLIM of NAD(P)H. J Biophotonics. 2018;11:e201800085.

[52] Li Z, Zhang X, Liu S, Zeng S, Yu L, Yang G, et al. BRG1 regulates NOX gene transcription in endothelial cells and contributes to cardiac ischemia-reperfusion injury. Biochim Biophys Acta Mol Basis Dis. 2018;1864:3477-3486.

[53] Reddy SS, Chauhan P, Maurya P, Saini D, Yadav PP, Barthwal MK. Coagulin-L ameliorates TLR4 induced oxidative damage and immune response by regulating mitochondria and NOX-derived ROS.

Toxicol Appl Pharmacol. 2016;309:87-100.

[54] Kahles T, Kohnen A, Heumueller S, Rappert A, Bechmann I, Liebner S, et al. NADPH oxidase Nox1 contributes to ischemic injury in experimental stroke in mice. Neurobiol Dis. 2010;40:185-192.

[55] De Silva TM, Brait VH, Drummond GR, Sobey CG, Miller AA. Nox2 oxidase activity accounts for the oxidative stress and vasomotor dysfunction in mouse cerebral arteries following ischemic stroke. PLoS One. 2011;6:e28393.

[56] Kleinschnitz C, Grund H, Wingler K, Armitage ME, Jones E, Mittal M, et al. Post-stroke inhibition of induced NADPH oxidase type 4 prevents oxidative stress and neurodegeneration. PLoS Biol. 2010;8:pii:e1000479.

Figures

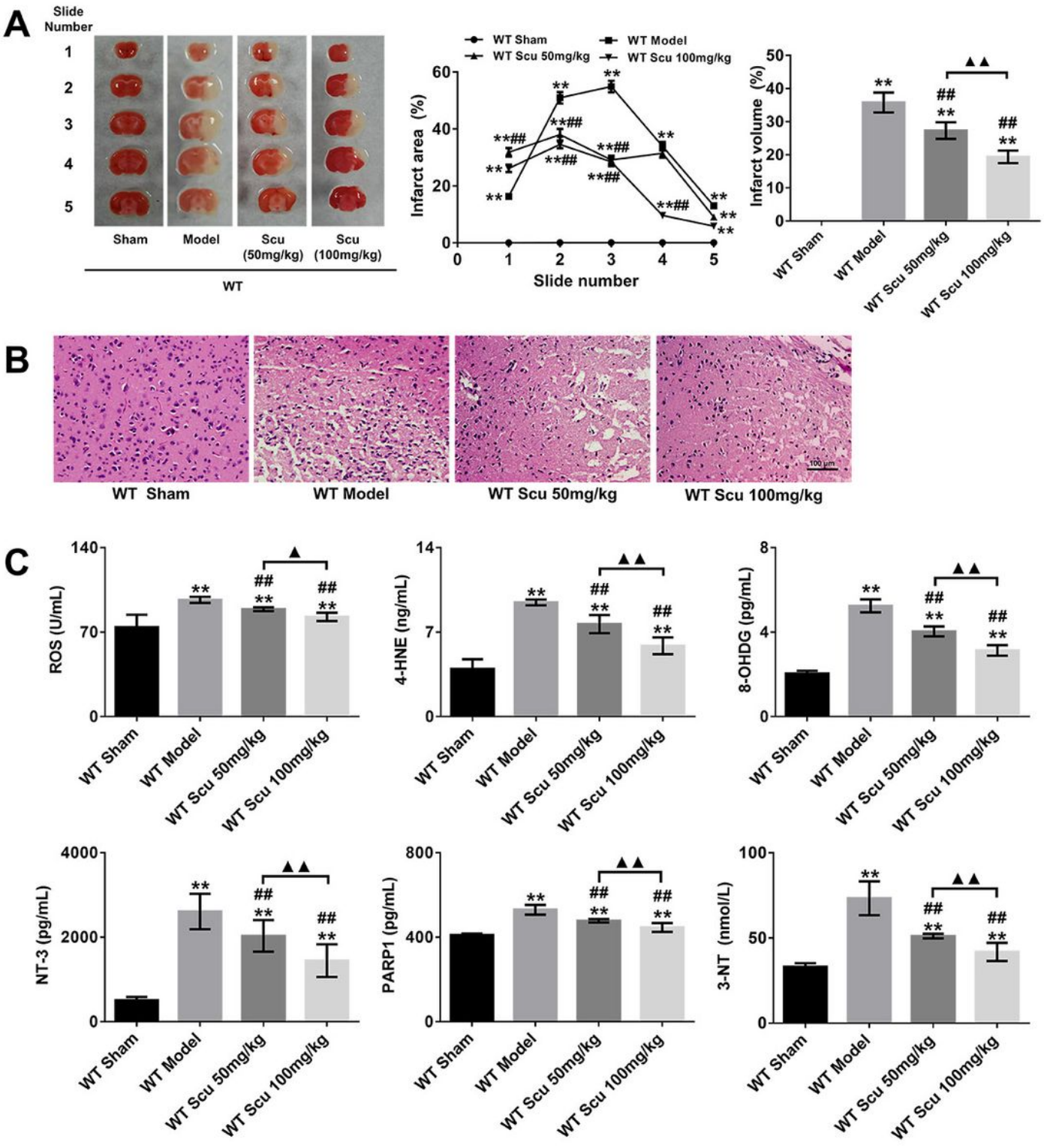

Figure 1

Scutellarin reduces ischemia-reperfusion injury by reducing oxidative factors in WT tMCAO mice. (A)TTC stained brain sections (n = 10),(B)HE staining of ischemic penumbra (n = 3, × 200),(C)ELISA detected the content of ROS, 4-HNE, 8-OHDG, NT-3, PARP1 and 3-NT in the ischemic penumbra of each group of WT mice (n = 7). **P<0.01 vs WT Sham; ## P<0.01 vs WT Model;▲▲P<0.01. Abbreviations:Scu, Scutellarin; WT, wild type; ROS, reactive oxygen species; 4-HNE, 4-hydroxynonenal; 8-OHDG, 8-

hydroxydeoxyguanosine; NT-3, neurotrophin-3; PARP1, poly ADP-ribose polymerase-1; 3-NT, 3-nitrotyrosine; TTC, 2,3,5-triphenyltetrazolium chloride; HE, hematoxylin-eosin; ELISA, enzyme-linked immunosorbent assay.

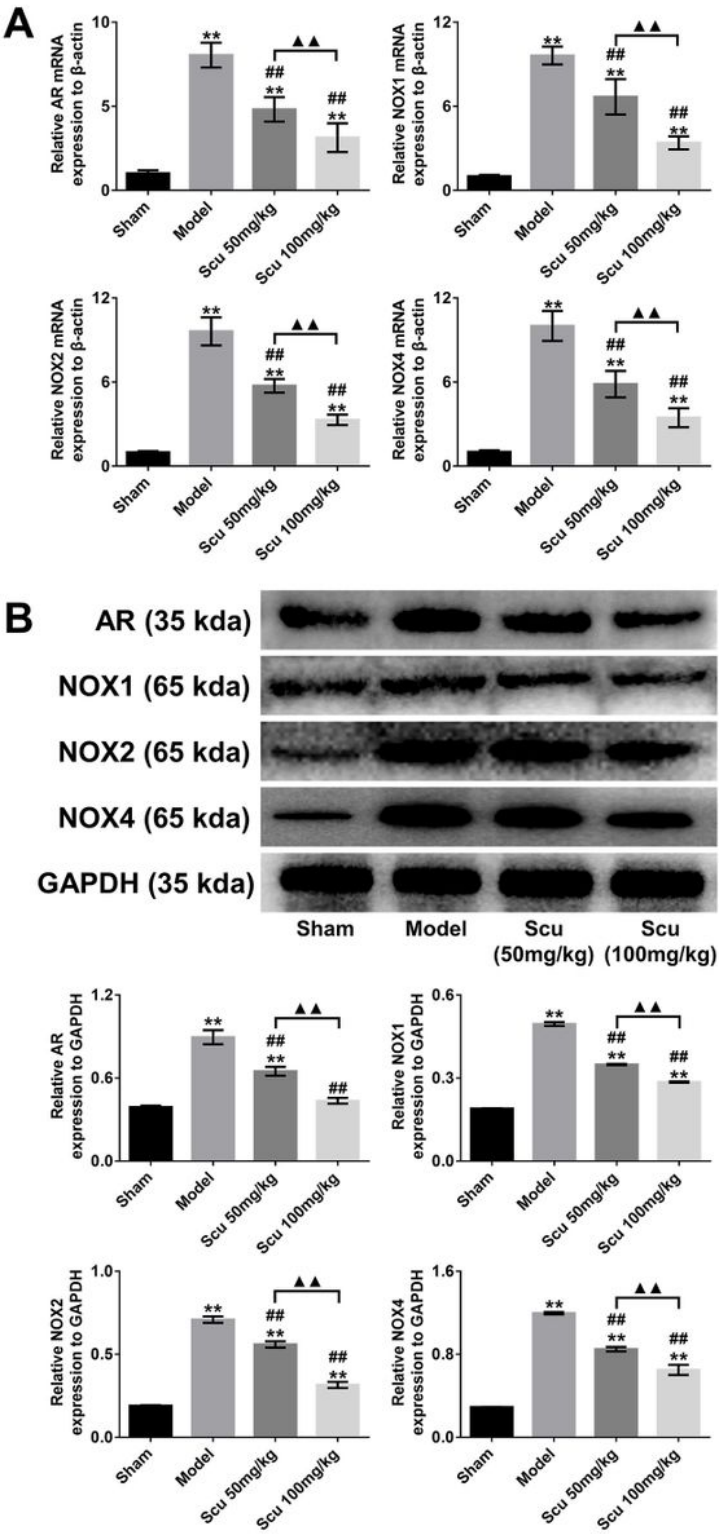

Figure 2

Scutellarin treatment reduced the expression of AR, NOX1, NOX2 and NOX4 in WT mice after tMCAO. (A)AR, NOX1, NOX2 and NOX4 mRNA expression by RT-RCR (n = 7),(B)AR, NOX1, NOX2 and NOX4 protein

expression by WB (n = 3). **P<0.01 vs WT Sham; ## P<0.01 vs WT Model; ▲▲P<0.01. Abbreviations:AR, aldose reductase; NOX, NADPH oxidase; WT, wild type; Scu, Scutellarin; RT-PCR, Real-time Polymerase chain reaction; WB, Western blot.

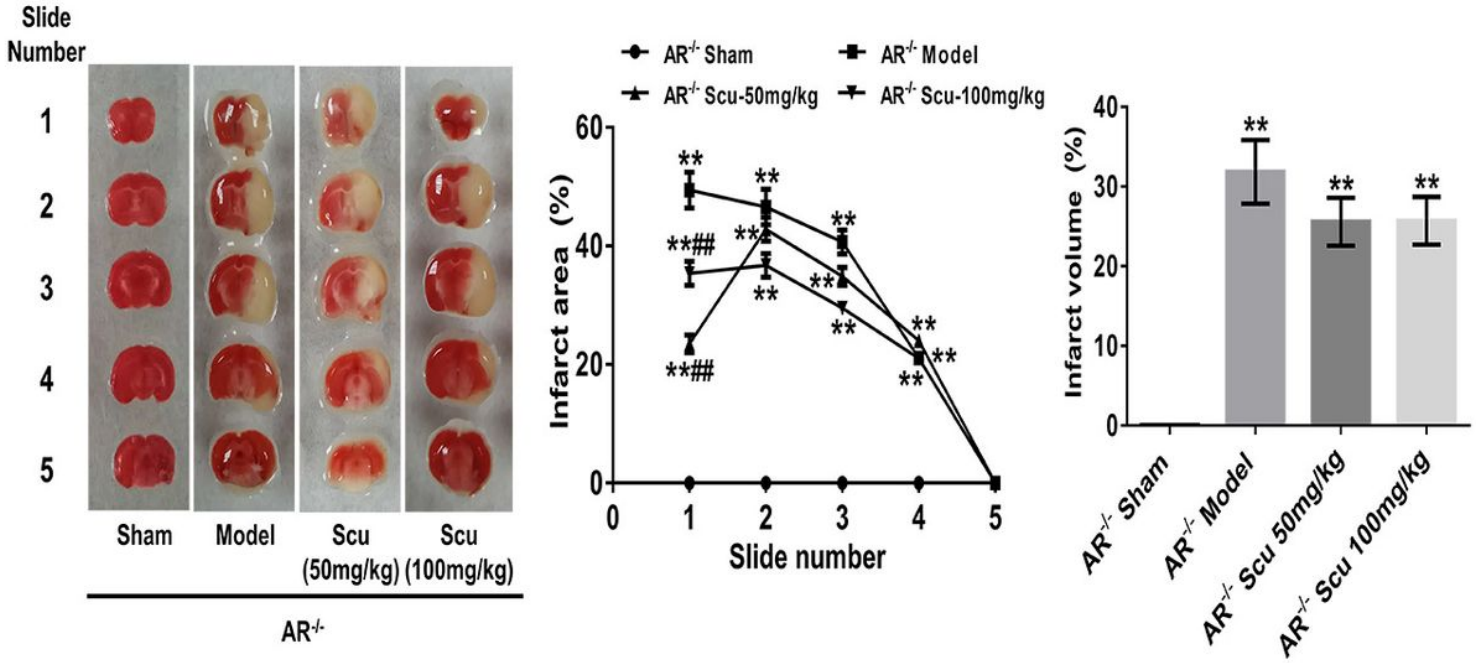

Figure 3

Scutellarin did not reduce the cerebral infarction area in AR-/- tMCAO mice. Scutellarin treatment had synergistic effects on the reduction of cerebral infarction area in AR-/- mice under ischemia cerebral injury by TTC (n = 10).**P<0.01 vs AR-/- Sham; ## P<0.01 vs AR-/- Model.Abbreviations:Scu, Scutellarin; AR, aldose reductase; TTC, 2,3,5-triphenyltetrazolium chloride.

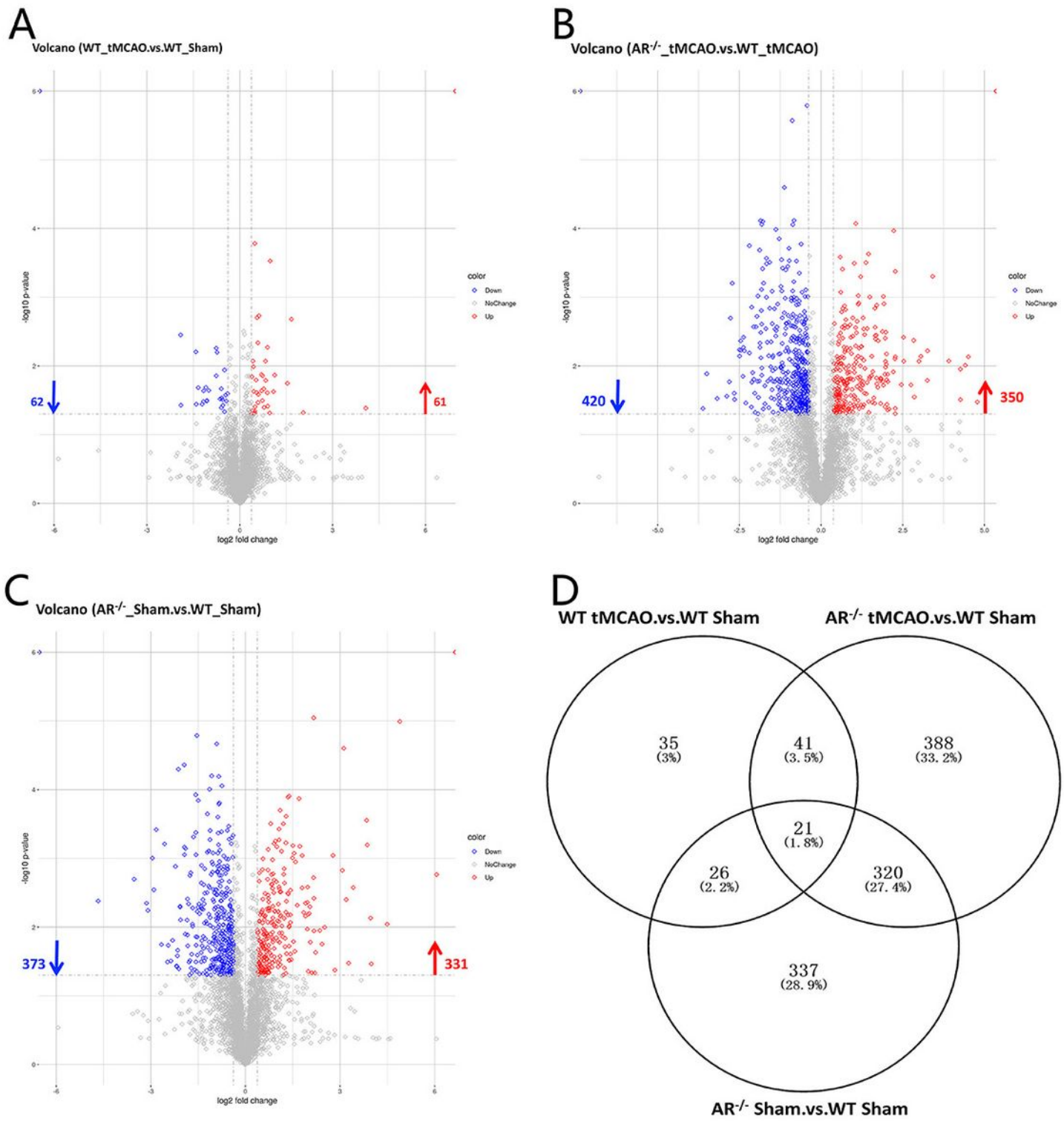

Figure 4

Different expressed proteins from Volcano diagram and Venn diagram in WT and AR-/- mice. The volcano plot illustrated the up- (red) and down-dysregulated (blue) DEPs from the comparison in WT sham group,WT tMCAO group,AR sham group and AR tMCAO group (A,B,C).The log2 fold-change (x axis) was plotted against the–log10 P-value (y-axis) (A,B,C).(A)Comparing WT tMCAO group with WT sham group,there are 61 up-regulations and 62 down-regulations in DEPs,(B)Comparing AR tMCAO group and

AR sham group DEPs have 350 up-regulations and 420 down-regulations,(C)Comparison between AR sham group and WT sham group, and there are 331 up-regulations and 373 down-regulations of DEPs, (D)Venn diagram between WT sham group, WT tMCAO group, AR sham group and AR tMCAO group.N=3.Abbreviations:DEPs, Different expressed proteins; WT, wild type; tMCAO, transient middle cerebral artery occluded; AR, aldose reductase.

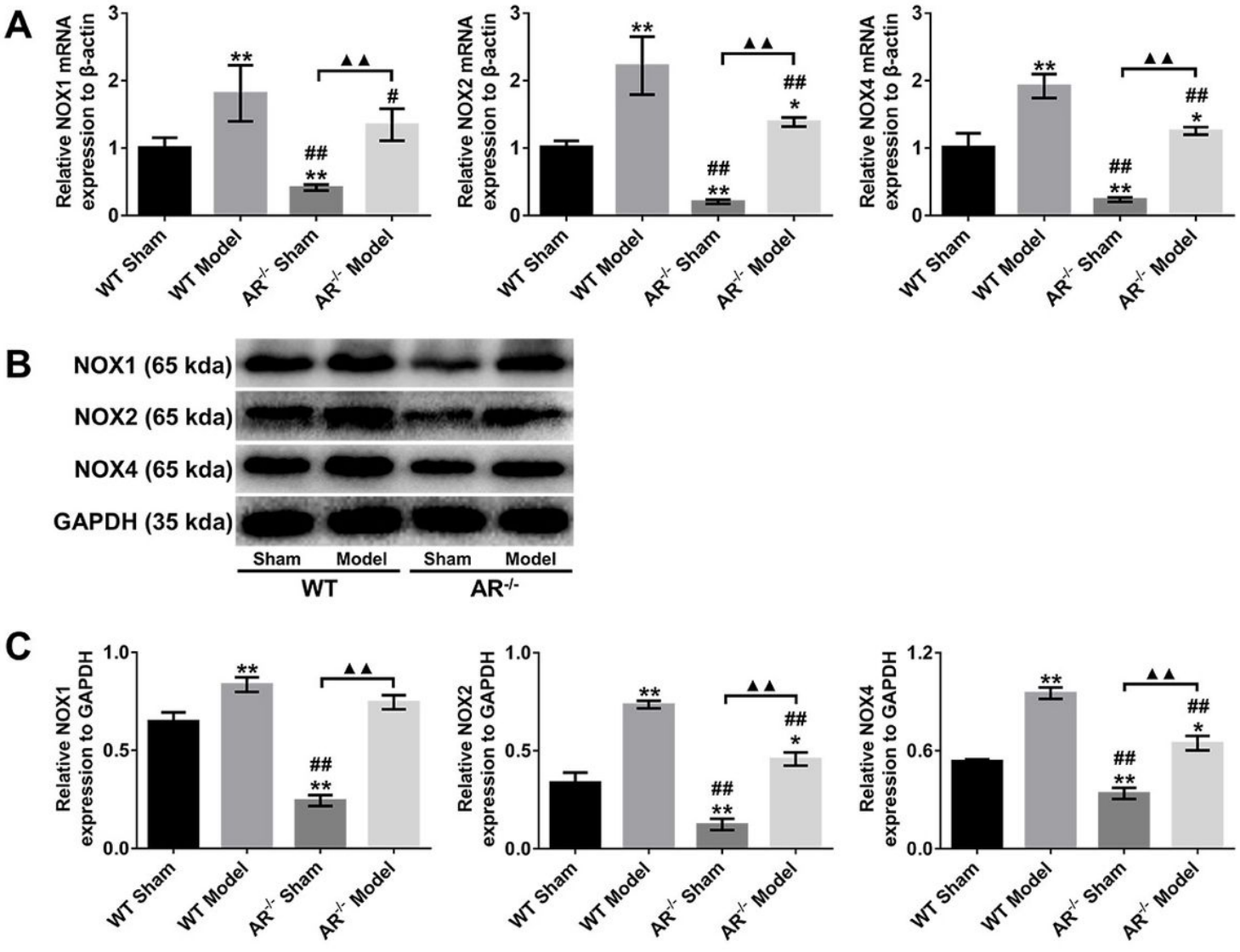

Figure 5

AR knockout decreased tMCAO induced NOX1、NOX2 and NOX4 mRNA and protein in mouse brain. The NOX1,NOX2 and NOX4 expressions in the AR-/- model group were significantly reduced compared with the WT model group (P <0.05).(A)the expression of NOX1, NOX2 and NOX4 mRNA in WT and AR-/- mice by RT-PCR (n = 7),(B)the expression of NOX1, NOX2 and NOX4 proteins in WT and AR-/- mice by WB (n = 3). *P<0.05, **P<0.01 vs WT Sham; #P<0.05, ## P<0.01 vs WT Model; ▲▲P<0.01.Abbreviations:NOX, NADPH oxidase; AR, aldose reductase; WT, wild type; RT-PCR, Real-time Polymerase chain reaction; WB, Western blot.

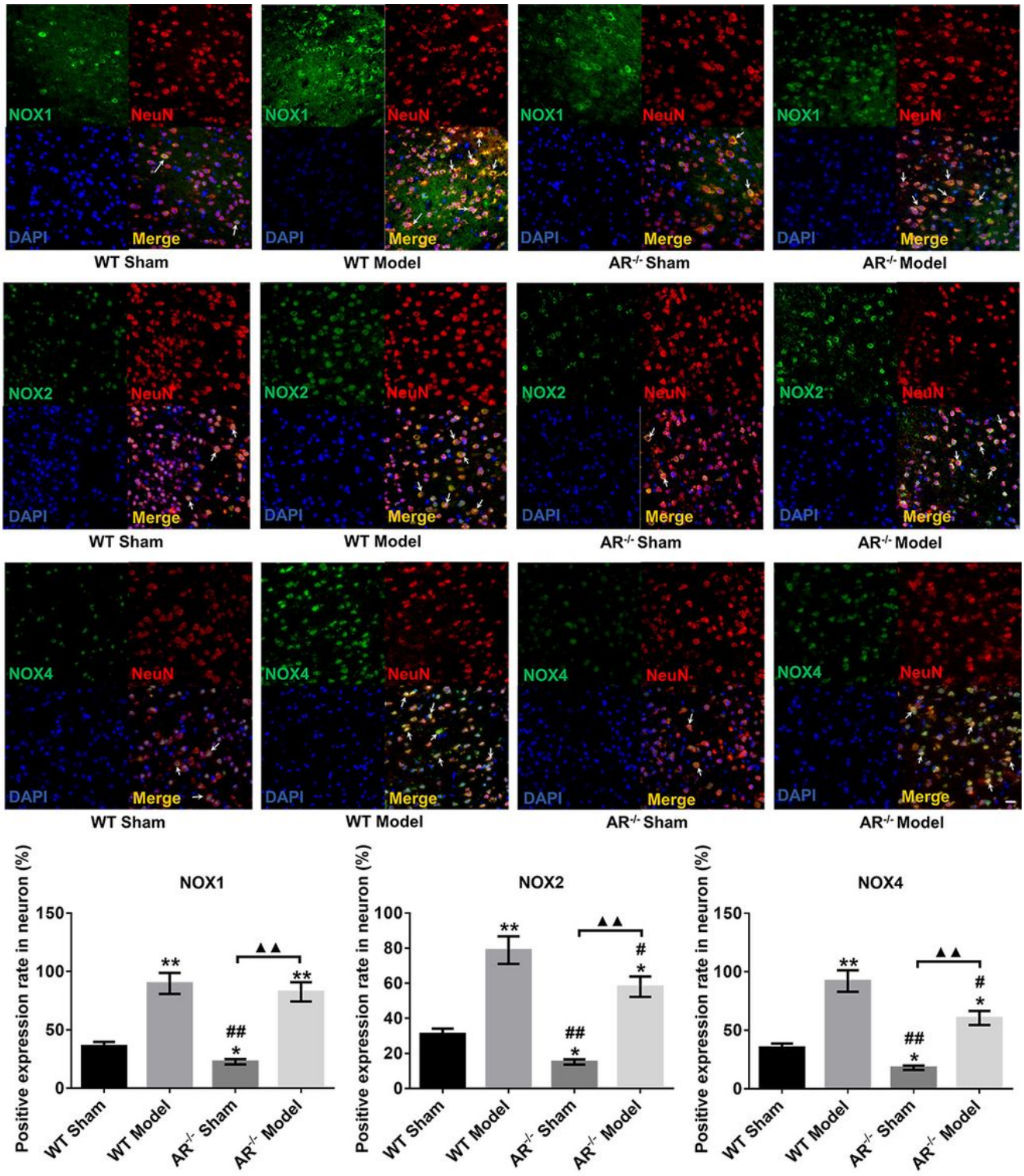

Figure 6

Comparison of NOX1, NOX2 and NOX4 protein expression in penumbra of WT and AR-/- tMCAO mice by immunofluorescence. The NOX1, NOX2 and NOX4 expressions in the AR-/- group were significantly reduced compared with the WT group (P <0.05).The NOX1, NOX2 and NOX4 expressions in the AR-/- sham group were significantly reduced compared with the AR-/- model group (P <0.01).N=3. Green is the positive expression of protein, which is marked by FITC. Red are neurons, marked by NeuN. Blue is the

nucleus, stained by DAPI.Yellow is positive expression in neurons.White arrows indicate some significant positive expressions.The scale bar is 50 μm.*P<0.05,**P<0.01 vs WT Sham; #P<0.05, ## P<0.01 vs WT Model;▲▲P<0.01.

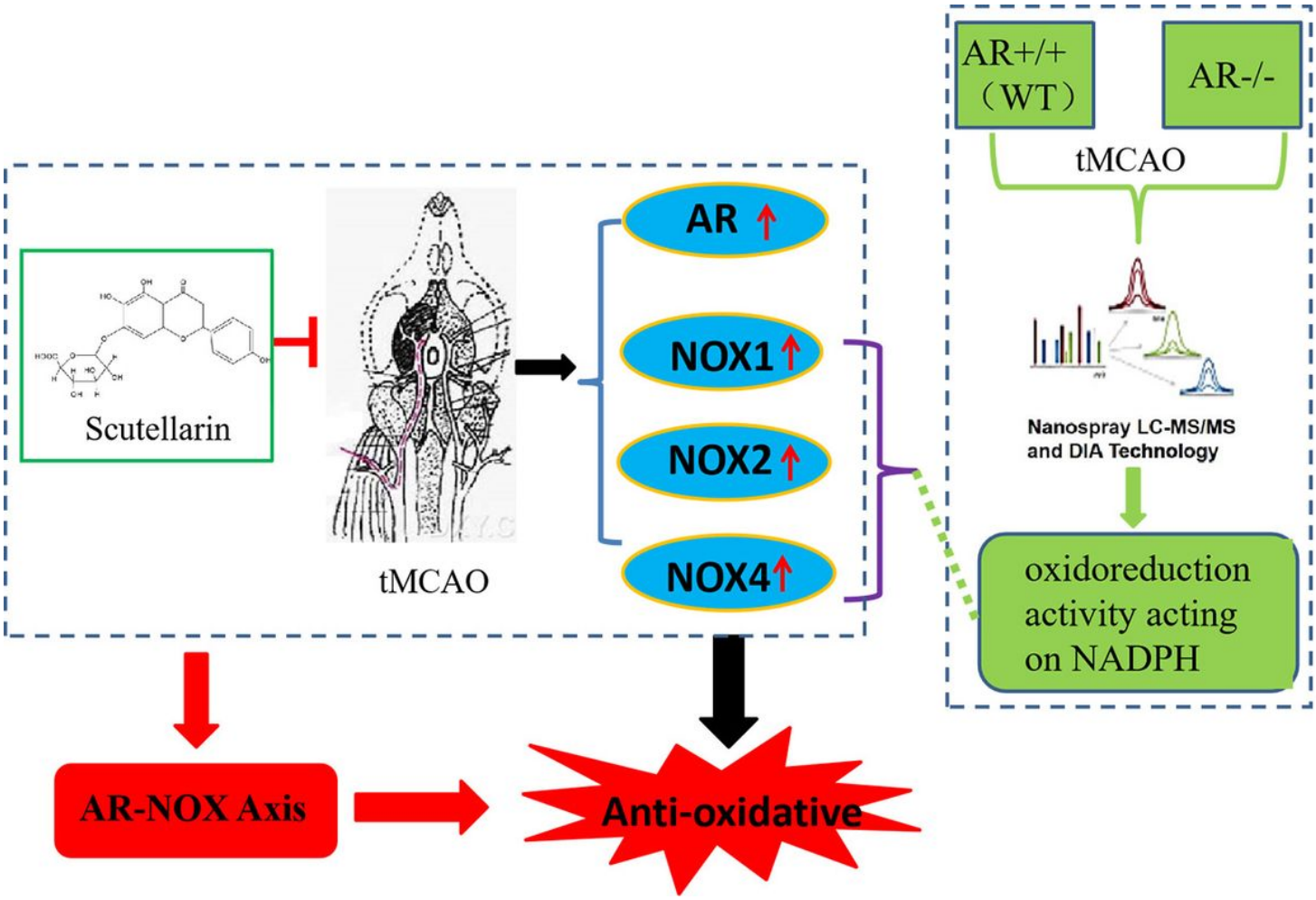

Figure 7

Scutellarin has the effect of inhibiting oxidative stress, and its target is aldose reductase. Scutellarin does not only down-regulate the expression of NOX2, but it also reduced other NOX isoforms such as NOX1 and NOX4 as well as associated oxidative injury markers after cerebral ischemia. Scutellarin also could down-regulated the expression of the AR gene.AR involvement in oxidative stress associated with cerebral ischemia and AR knockout leads to protection against cerebral ischemic injury. As a result, we think that the protective effects of Scutellarin on ischemic stroke is through the AR-NOX axis to modulate the oxidative stress injury.

Supplementary Files

This is a list of supplementary files associated with this preprint. Click to download.

- AdditionalfilesFigS1.tif
- AdditionalfilesFigS2.tif

- AdditionalfilesFigS3.tif
- AdditionalfilesTableS1.xlsx
- AdditionalfilesTableS2.xlsx
- AdditionalfilesTableS3.xlsx
- AdditionalfilesTableS4.xlsx